# Programmable organic thin-film devices with extremely high current densities

Troy Graves-Abe[a] and J. C. Sturm
*Department of Electrical Engineering, Princeton Institute for the Science and Technology of Materials (PRISM), Princeton University, Princeton, New Jersey 08544*

(Received 21 February 2005; accepted 2 August 2005; published online 20 September 2005)

Thin (12 nm) organic films consisting of self-assembled multilayers of 11-mercaptoundecanoic acid were contacted by gold electrodes. The devices could be operated as a programmable memory by applying low-voltage pulses to increase the conductivity by $10^3$ and then high-voltage pulses to reverse the increase; the conductivity of the stored state could be read nondestructively by applying a still-lower voltage pulse. Programmed states remained stable for longer than three months and devices were functional for more than $10^4$ programming cycles. Current-voltage measurements of the devices revealed negative differential resistance with enormous current densities characteristic of metallic conduction (up to $10^7$ A/cm$^2$). These results are promising for application in dense, high-speed memory arrays, where resistance-capacitance delays can be minimized by large current densities. © *2005 American Institute of Physics*. [DOI: 10.1063/1.2058219]

There is growing interest in using organic devices as electronic memory elements.[1,2] A variety of promising approaches, including reconfigurable and redox-active molecules,[3–6] charge-trapping,[7–9] write-once mechanisms,[10] and others,[11–15] have recently been demonstrated. Much of this research has been driven by the desire for high-speed and high-density (low-cost) memory that is nonvolatile (i.e., retains its state when power is removed). A fundamental challenge in satisfying the demands for both high speed and density is that resistance-capacitance delays increase rapidly as the capacitance between metal interconnect lines is increased when they are fabricated in high-density arrays. High current densities are desirable to overcome these delays and for fast signal processing.[10] In this work, we report that devices consisting of self-assembled multilayers of the insulating molecule 11-mercaptoundecanoic acid (MUA) display nonvolatile, programmable conductance switching and negative differential resistance (NDR) with extremely high current densities (up to $10^7$ A/cm$^2$). These current densities are higher than those reported in the previous studies by $10^4$ and suggest that a switchable, metallic-type conduction is occurring in the films. Electronic devices comprised of these films are therefore attractive candidates for nonvolatile memory with high density and speed.

The devices were fabricated using both edge and planar structures [Figs. 1(a) and 1(b)]. In the edge structure, a self-aligned, insulating layer of silicon oxide ($SiO_x$) deposited on a Au electrode was used to limit the device to the vertical area on the edge of the Au film [Fig. 1(a)]. Details of the structure fabrication are reported elsewhere.[16] Briefly, trenches were etched into a Si wafer to define mesas, onto which self-aligned layers of Au (25 nm) and $SiO_x$ (40 nm) were deposited (with 5 nm Ti layers for adhesion). Multiple layers of MUA (typically 7–8 layers, to a total thickness of ~12 nm) were then self-assembled on the exposed edge of the Au film by alternating immersions of the sample in dilute (~1 mM) solutions of MUA and $Cu(ClO_4)_2$ in ethanol. The samples were left in the MUA solution for 3 to 10 h to grow a monolayer of MUA, then exposed to the $Cu(ClO_4)_2$ solution for 5 min to add a layer of copper ions. Between immersions, the samples were rinsed thoroughly in ethanol after $Cu(ClO_4)_2$ exposure, or ethanol and deionized water after MUA exposure. This procedure, which is described in more detail elsewhere,[17] was repeated to yield bilayers of MUA and copper. After the MUA growth, a second Au layer was then deposited on top of the organic film (with the sample held at low temperatures near 100 K to avoid thermal damage to the organic layer[18]) to define the second electrode. The active device area, limited to the edge of the first Au film by the $SiO_x$ layer, is typically $10^{-9}$ cm$^2$.

In the planar structure, a layer of Au (80 nm, with a 5 nm Ti layer for adhesion) was deposited onto a Si substrate. After MUA growth on the Au film, a patterned layer of $SiO_x$ (70 nm) was deposited through a shadow mask. Finally, another Au layer was deposited through a second shadow mask with the sample held at low temperatures. The $SiO_x$ layer provides a rigid platform so that the second Au layer can be contacted by a needle probe for electrical measurements without damaging the MUA while, most significantly, minimizing the device active area to avoid pinholes leading to shorted devices [Fig. 1(b)]. These planar devices typically

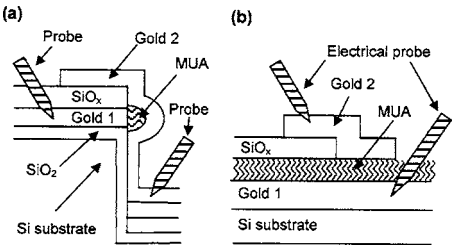


FIG. 1. (a) Schematic of the edge structure. The active device area is defined by the thickness of the first gold layer on which the MUA self-assembles and the width of the second, shadow-masked gold layer (25 nm $\times$25 $\mu$m). The electrical characteristics can be probed through large-area contact pads (25$\times$50 $\mu$m). (b) Schematic of the planar structure. The active device area (where the gold electrodes overlap with no $SiO_x$ present) is typically 200 $\mu$m$^2$. The device can be contacted through probe areas (typically >1000 $\mu$m$^2$) on top of and adjacent to the $SiO_x$ layer.

[a]Electronic mail: tabe@princeton.edu

 

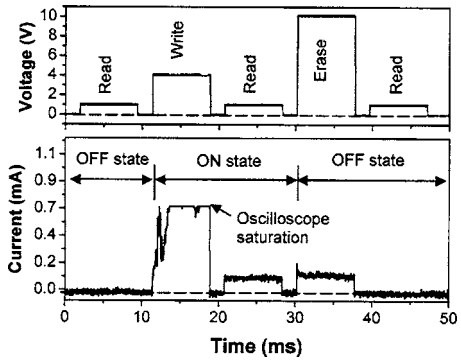


FIG. 2. Typical programming sequence for 11 nm MUA film in edge structure where applied voltage pulses for programming (4 or 10 V for write or erase operations, respectively) are alternated with 1-V pulses to read the state of the device. The current during the write pulse (actually ~1.2 mA) exceeds the measurement range of the oscilloscope and is cutoff.

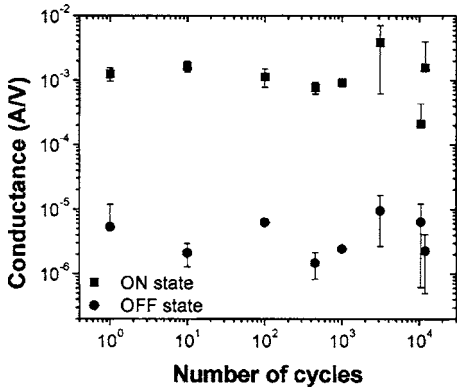


FIG. 3. Evolution of the conductance (measured at 1 V) of ON and OFF memory states following multiple write/erase cycles. The device consists of an 11 nm thick MUA film in the edge structure. The write pulse was 4 V, 8 ms, and the erase pulse was 10 V, 1.5 ms. Error bars represent variations in conductance measured in four consecutive write/erase cycles.

had relatively large device areas of $10^{-6}$ cm$^2$.

MUA is fundamentally an insulating molecule, consisting of an alkane chain terminated by thiol and carboxyl groups. As expected, most MUA films were initially insulating, with current densities at 1 V applied bias that ranged from $10^{-3}$ to $10^{-1}$ A/cm$^2$ (edge devices[16]) or $10^{-6}$ to $10^{-3}$ A/cm$^2$ (planar devices). After scanning the voltage above 6.5 V, the low-voltage conductivity of the "burned-in" devices increased by $10^2$ to $10^4$. The devices could then be programmed into high- and low-conductivity states by the application of short (several ms) voltage pulses.

A typical programming sequence on an edge device is shown in Fig. 2 (qualitatively similar characteristics were observed in both structures). For simplicity, we define programming into the ON state as a "write" operation, and programming into the OFF state as an "erase" operation. Initially, the device is in the OFF state so that the 1 V, 7 ms "read" pulse causes a current in the microamp range. Next, a 4 V write pulse is applied. The subsequent read pulse measures a current of 100 $\mu$A (corresponding to a current density of $2\times10^4$ A/cm$^2$) in the ON state, 100 times higher than the OFF state. A 10 V erase pulse then returns the device to the OFF state that is read by the final 1 V pulse. Characteristics were independent of voltage bias so that writing and erasing could be achieved with both positive and negative voltages. Programmed states remained stable for longer than three months with no applied voltage in an inert atmosphere. Preliminary measurements of the transient switching behavior suggest that the device can be switched into the OFF state in less than 50 ns, although the ON state may take several ms to program. Devices could endure many programming cycles without degrading (Fig. 3). A ratio of ~$10^3$ between the high- and low-conductivity states was maintained through $10^4$ write/erase cycles.

In the edge devices, the conductance per unit area (measured at 1 V) of the ON state was $10^4$ to $10^5$ S/cm$^2$. This high conductance per unit area is desirable for fast, low-noise data readouts in integrated circuit memory. Qualitatively similar electrical characteristics to those reported here have been observed previously, originally in electroformed inorganic films,[19–23] though most recently in 100 nm organic films [aluminum tris(8-hydroxyquinoline) containing a thin layer of metallic nanoclusters[8]]. In contrast to our devices, previous workers typically report devices that we calculate have conductances per unit area at 1 V applied bias of less than 1 S/cm$^2$, over four orders of magnitude lower than observed here. Additionally, a number of other (mostly reversible) nonvolatile memory devices comprised of polymeric, small-molecule, or self-assembled organic films have been demonstrated; but again from the published data we estimate relatively low conductances per unit area ($10^{-8}$ to $10^2$ S/cm$^2$) in the 0.1 to 1 V range.[4–15]

Most authors have attributed the reversible conductivity in electroformed devices to one of two models. In the first, conducting paths are formed in the film at voltages between 3–5 V, causing the device to enter its high-conductivity state; these paths are destroyed at higher voltages, leading to the low-conductivity state.[20,24,25] In the second model, charges trapped within the film tend to be released at voltages between 3 and 5 V, resulting in higher conductances; at higher voltages charges are more likely to be trapped, causing an electric field that suppresses current.[8,19,26] It is not likely that charge trapping is the mechanism in our work because the effect is also observed in devices with only three MUA layers (4 nm thick). Any trapped charge in this case would readily tunnel through the organic film. The conducting path model is therefore considered more relevant to this work. Whether the conductive paths are primarily metallic or have a more complicated structure is currently under investigation.

We also note that by applying a swept voltage to the devices, symmetric NDR with a peak between 2.5 and 4 V for both positive and negative voltages on the top electrode could be observed (Fig. 4). Large peak-to-valley ratios of up

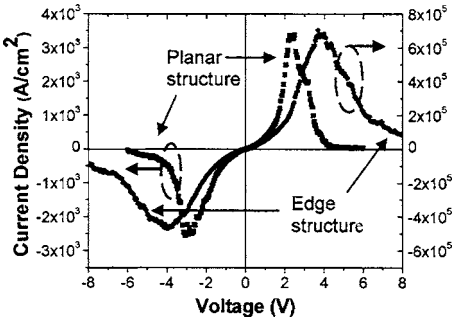


FIG. 4. (A) Current-density vs voltage (with applied voltage) of 11 nm MUA films in planar (left vertical axis) and edge structures (right vertical axis). The voltage was scanned from negative to positive at 2 V/s.

to 140:1 were observed, although ratios of ~10:1 were more common. The current-voltage characteristics of both structures were qualitatively similar; however, much higher current densities were typically observed in the edge structures. In these structures, the average peak current density was $3 \times 10^6$ A/cm$^2$, but devices with peak current densities in excess of $10^7$ A/cm$^2$ were measured. The most studied family of devices in which NDR is observed consists of tunneling diodes. In these devices the NDR characteristics are due to enhanced charge tunneling through a barrier when energy levels adjacent to the barrier are aligned by a bias voltage (without storage of a nonvolatile state). In our devices, the NDR instead reflects a dynamic programming of the device into the high-conductivity ON state as the voltage is swept between 2.5 to 5 V, then a second programming phase to return the device to the low-conductivity OFF state at higher voltages. We have also performed experiments in which the top gold electrode is replaced by aluminum.[27] In these experiments, NDR is observed only for positive bias on the gold electrode, suggesting that the electrical characteristics are dependent on gold ions injected from the electrode and not the copper ions interspersed in the MUA layer during the self-assembly process.

To confirm that the MUA layer is necessary to observe the reported electrical characteristics, control devices were fabricated without the MUA layer or with the second Au electrode overlapping only the $SiO_x$ layer. In both structures, devices without the MUA layer were shorted, and when the electrodes overlapped over only the $SiO_x$ layer, insulating characteristics were measured. However, in devices with an MUA film, the electrical characteristics depended only weakly on the number of MUA layers. Current densities decreased slightly, by a factor of 10, as the number of MUA layers was increased from 4 to 12 (6 to 20 nm thickness) for both edge and planar devices. In contrast, the low-voltage ($<2$ V) currents in pristine devices (prior to the forming step) decreased exponentially with the number of MUA layers in the device, with a slope of one decade per 1.8 layers of MUA. We also note that as the number of MUA layers was decreased below 4, very few operable devices could be found, and for devices with 1 to 2 MUA layers no working devices were observed.

Close inspection of the devices after electrical testing with a scanning electron microscope revealed a roughening of the top metal layer, which may be related to the formation of the metallic, conducting paths to which we attribute the observed electrical characteristics. This roughening was more apparent in devices with the planar structure. The lower current density in the planar structure (almost $10^3$ less than in the edge structure) may be a result of this increased roughness leading to a decreased effective device area.

In summary, electrically programmable conductivity switching with extremely low ON resistance was observed. This appears to be due to the creation and destruction of conducting paths in the MUA film. This phenomenon leads to NDR in the current-voltage characteristics, with peak current densities as high as $10^7$ A/cm$^2$. The high current densities and multiple programming cycles that can be achieved in these devices suggest much promise for potential application as high-speed memory elements.

This work was supported by ONR contract N00014-02-1-075 and the New Jersey Center for Organic Optoelectronics.

[1] C.-U. Pinnow and T. Mikoajick, J. Electrochem. Soc. **151**, K13 (2004).
[2] Y. Yang, L. P. Ma, and J. Wu, MRS Bull. **29**, 833 (2004).
[3] Z. Liu, A. A. Yasseri, J. S. Lindsey, and D. F. Bocian, Science **302**, 1543 (2003).
[4] A. Bandyopadhyay and A. J. Pal, Appl. Phys. Lett. **82**, 1215 (2003).
[5] J. Chen and M. A. Reed, Chem. Phys. **281**, 127 (2002).
[6] Y. Luo, C. P. Collier, J. O. Jeppesen, K. A. Nielsen, E. Delonno, G. Ho, J. Perkins, H.-R. Tseng, T. Yamamoto, J. F. Stoddart, and J. R. Heath, ChemPhysChem **3**, 519 (2002).
[7] L. P. Ma, J. Liu, and Y. Yang, Appl. Phys. Lett. **80**, 2997 (2002).
[8] L. D. Bolzano, B. W. Kean, V. R. Deline, J. R. Salem, and J. C. Scott, Appl. Phys. Lett. **84**, 607 (2004).
[9] J. Ouyang, C.-W. Chu, C. R. Szmanda, L. P. Ma, and Y. Yang, Nat. Mater. **3**, 918 (2004).
[10] S. Möller, S. R. Forrest, C. Perlov, W. Jackson, and C. Taussig, J. Appl. Phys. **94**, 7811 (2003).
[11] L. P. Ma, Q. Xu, and Y. Yang, Appl. Phys. Lett. **84**, 4908 (2004).
[12] H. J. Gao, K. Sohlberg, Z. Q. Xue, H. Y. Chen, S. M. Hou, L. P. Ma, X. W. Fang, S. J. Pang, and S. J. Pennycock, Phys. Rev. Lett. **84**, 1780 (2000).
[13] T. Oyamada, H. Tanaka, K. Matsushige, H. Sasabe, and C. Adachi, Appl. Phys. Lett. **83**, 1252 (2003).
[14] J. H. Krieger, S. V. Trubin, S. B. Vaschenko, and N. F. Yudanov, Synth. Met. **122**, 199 (2001).
[15] D. M. Taylor and C. A. Mills, J. Appl. Phys. **90**, 306 (2001).
[16] T. Graves-Abe, Z. Bao, and J. C. Sturm, Nano Lett. **4**, 2489 (2004).
[17] S. D. Evans, A. Ulman, K. E. Goppert-Berarducci, and L. J. Gerenser, J. Am. Chem. Soc. **113**, 5866 (1991).
[18] C. Zhou, M. R. Deshpande, M. A. Reed, L. Jones II, and J. M. Tour, Appl. Phys. Lett. **71**, 611 (1997).
[19] J. G. Simmons and R. R. Verderber, Proc. R. Soc. London, Ser. A **301**, 77 (1967).
[20] G. Dearnaley, A. M. Stoneham, and D. V. Morgan, Rep. Prog. Phys. **33**, 1129 (1970).
[21] A. K. Ray and C. A. Hogarth, Int. J. Electron. **57**, 1 (1984).
[22] D. P. Oxley, R. E. Thurstans, and P. C. Wild, Thin Solid Films **20**, 23 (1974).
[23] M. G. Lopez and R. D. Gould, Thin Solid Films **333**, 170 (1998).
[24] S. Gravano, E. Amir, R. D. Gould, and M. Abu Samra, Thin Solid Films **433**, 321 (2003).
[25] A. K. Ray and C. A. Hogarth, Int. J. Electron. **69**, 97 (1990).
[26] R. E. Thurstans and D. P. Oxley, J. Phys. D **35**, 802 (2002).
[27] T. Graves-Abe and J. C. Sturm, Mater. Res. Soc. Symp. Proc. **871E**, I9.34 (2005).